

# Enabling FDD Massive MIMO through Deep Learning-based Channel Prediction

Maximilian Arnold, Sebastian Dörner, Sebastian Cammerer, Sarah Yan,  
Jakob Hoydis, and Stephan ten Brink.

## Abstract

A major obstacle for widespread deployment of frequency division duplex (FDD)-based Massive multiple-input multiple-output (MIMO) communications is the large signaling overhead for reporting full downlink (DL) channel state information (CSI) back to the basestation (BS), in order to enable closed-loop precoding. We completely remove this overhead by a deep-learning based channel extrapolation (or “prediction”) approach and demonstrate that a neural network (NN) at the BS can infer the DL CSI centered around a frequency  $f_{DL}$  by solely observing uplink (UL) CSI on a different, yet adjacent frequency band around  $f_{UL}$ ; no more pilot/reporting overhead is needed than with a genuine time division duplex (TDD)-based system. The rationale is that scatterers and the large-scale propagation environment are sufficiently similar to allow a NN to learn about the physical connections and constraints between two neighboring frequency bands, and thus provide a well-operating system even when classic extrapolation methods, like the Wiener filter (used as a baseline for comparison throughout) fails. We study its performance for various state-of-the-art Massive MIMO channel models, and, even more so, evaluate the scheme using actual Massive MIMO channel measurements, rendering it to be practically feasible at negligible loss in spectral efficiency when compared to a genuine TDD-based system.

## I. INTRODUCTION

With a significant increase in area throughput, Massive multiple-input multiple-output (MIMO) antenna communication has become an enabling technology for the upcoming fifth generation (5G) wireless mobile communication systems [1], [2], [3], [4]. However, Massive MIMO systems described in current research literature commonly exploit channel reciprocity and hence rely on time division duplex (TDD)-based approaches [1], i.e., uplink (UL) and downlink (DL) channels share the *same* frequency band in orthogonal time intervals. Achieving such reciprocity in practice requires accurate hardware with costly calibration circuitry. To mitigate this issue, various alternatives to a full Massive MIMO system have been proposed such as the *grid of beams* [5] and codebook Massive MIMO [6]. As frequency division duplex (FDD) does not rely on channel reciprocity, it is a practically highly relevant topic, and both academia and industry have been striving for enabling FDD Massive MIMO. However, it is widely accepted as a fundamental limitation that FDD Massive MIMO has a prohibitive high piloting/reporting overhead related to channel estimation in both UL and DL direction [1], unless certain conditions on the channel covariance structure are satisfied which, however, are rarely observed in practice [7], [8]. In TDD, the user equipment (UE) sends a single pilot symbol to its  $M$  antennas at the basestation (BS), allowing the BS to estimate the UL channels in one time slot, and, by exploiting channel reciprocity, to re-use these UL channel estimates for precoding in the DL, without the need for any costly channel state information (CSI) reporting feedback. However, in FDD systems, this reciprocity does not hold from one

M. Arnold, S. Dörner, S. Cammerer, S. Yan, and S. ten Brink are with the Institute of Telecommunications, University of Stuttgart, Pfaffenwaldring 47, 70659 Stuttgart, Germany, {arnold,doerner,cammerer,tenbrink}@inue.uni-stuttgart.de)

J. Hoydis is with Nokia Bell Labs, Route de Villejust, 91620 Nozay, France, jakob.hoydis@nokia-bell-labs.com.

frequency band to another and, thus, the DL channels from each antenna to the UE must be estimated separately, and reported back to the BS, incurring an overhead proportional to the number of antennas  $M$  [1].

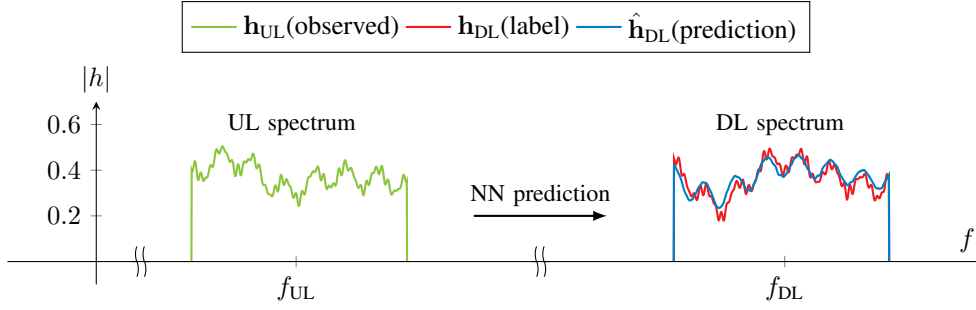


Fig. 1: Using the uplink CSI at  $f_{UL}$  to infer on downlink CSI at  $f_{DL}$ .

On the other hand, FDD Massive MIMO promises compatibility to current frequency allocations for mobile communication systems and, potentially, reduces latency [9]. It has been shown that a compressed sensing approach [10] achieves almost the same minimal piloting overhead as TDD Massive MIMO. However, it is unclear whether the general assumption of channel sparsity holds in practice [7], [11]. Other approaches such as [12], [13] rely on an underlying channel model including expert knowledge on the antenna geometry. Further, the authors in [14] propose a super-resolution channel estimation via deep learning in such a way that the neural network (NN) interpolates subcarriers without pilots from neighboring subcarriers. In [15] it was proposed to replace an orthogonal frequency division multiplex (OFDM) channel estimation combined with data detection by a NN. Recently, different CSI prediction approaches exploiting channel sparsity have been proposed in [16], [17]. Another particular interesting idea to reduce the piloting overhead by using a subset of antennas to predict the remaining antennas was introduced in [18]. While this approach aims at predicting the channel at a different spatial location, but on the same frequency, we try, in this work, to estimate the channel at a different frequency but for the same spatial position. However, none of these works focus on the problem of extrapolating/prediction from one frequency band to an adjacent frequency band and, to the best of our knowledge, no general solution for the FDD Massive MIMO problem is known. A *classical* estimation using the channel covariance matrix, which has not resulted a practical solution yet, was approached in [6], [19]. Although machine learning and, in particular, deep learning has attracted a lot of attention for a wide variation of different communication applications, it currently lacks of solutions showing practical gains. One important contribution of our work is to show that a NN can *enable* solutions (i.e., FDD CSI extrapolation/prediction) for which simply no satisfactory *classical* signal processing algorithm is known, or, even more so, where classic approaches (Wiener filter) would fail.

In this work, the general idea is to estimate the DL CSI only based on the observed UL CSI via deep NNs and, thus, overcome a major practical limitation for FDD Massive MIMO. Our approach works for any considered scenario with adjacent frequency bands and, in contrast to compressed sensing, does not rely on channel sparsity as it also works in the single-input single-output (SISO) scenario. The intuition behind this prediction scheme is that the impinging waves at the UE, generated through different scatterers, are assumed to be similar over a small frequency bandwidth, although it may be hard to describe the connection in terms of an analytical model. Therefore, a NN should be able to *approximate* such a function without the need of any a priori knowledge other than the observed measured data. Fig. 1 illustrates the proposed scheme for an OFDM system, extrapolating CSI from a frequency band centered around  $f_{UL}$  to a nearby frequency band centered around  $f_{DL}$ .

This ease in modeling and flexibility in application comes at the cost of acquisitioning large quantities of channel estimates, plus retraining whenever the radio environment changes significantly. We believe, however, that data acquisition is not a real

limitation, as a hybrid approach could use pilots whenever the BS operates at low average load without any additional effort, allowing the continuous refinement of the NN weights; only during high load periods the BS may switch to the proposed CSI prediction scheme. Also, the training could be outsourced to a datacenter and only the updated weights need to be transmitted to the BS whenever a performance improvement can be achieved.

In a first step, we analyze the proposed scheme with the help of several simple examples, such as the SISO setting to demonstrate the general feasibility of CSI prediction from UL to DL in the SISO scenario. This provides important insights into designing and training a NN for such a signal processing task, and also allows the comparison within an analytical setup. Next, standardized channel models such as the 3GPP 38.901 channel model (implemented by the Quadriga framework [20]) and measurements are evaluated to show the viability of our proposed setup in a realistic setting. Furthermore, with our measurements we show that the spectral efficiency loss in a practical system with 32 antennas is rather moderate ( $\sim 10\%$  in line-of-sight (LoS),  $\sim 20\%$  in non-line-of-sight (NLoS)), rendering our scheme to be an attractive proposition for future wireless communication systems.

The remainder of this paper is structured as follows: Section II starts with fundamental limitations of FDD Massive MIMO and discusses different metrics needed to evaluate predicted CSI. Section III provides a short introduction to deep learning and clarifies notation. In Section IV, we introduce the proposed NN-based approach for the SISO scenario, provide results for simulated and measured scenarios and compare the NN's performance to a Wiener filter-based approach, i.e., *the* classic signal processing baseline. The simulations and measurements are then extended to a Massive MIMO scenario in Section V; finally Section VI concludes the paper.

*Notations:* Boldface letters and upper-case letters denote column vectors and matrices, respectively. The  $i$ th element of vector  $\mathbf{x}$  is denoted  $x_i$ . The notation  $\mathbf{x}^H$  denotes the Hermitian transpose of  $\mathbf{x}$ .

## II. SYSTEM MODEL AND FUNDAMENTAL LIMITATIONS

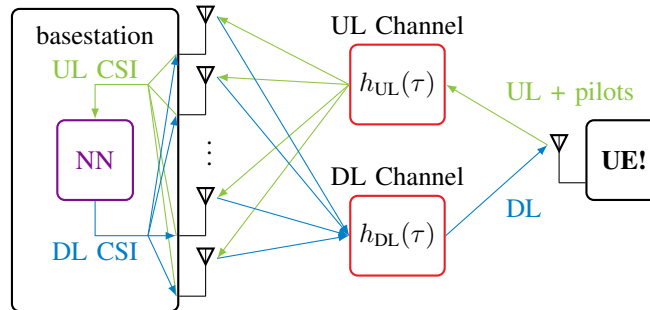


Fig. 2: The DL CSI extrapolation is based on a NN trained using UL CSI observations.

Fig. 2 depicts the fundamental problem we tackle in this work. The task of the BS is to estimate the DL CSI  $h_{DL}(\tau)$  only by observing the UL CSI  $h_{UL}(\tau)$  (UL pilots) as shown in Fig. 2.<sup>1</sup> Obviously, the success of such an approach relies on whether there is an underlying physical relation between the considered frequency bands; thus, in Section IV and Section V, respectively, we demonstrate the validity of this assumption for both simulated and measured scenarios.

<sup>1</sup>We consider a scenario where the BS has multiple antennas, while each UE has a single antenna. Extensions to UEs with multiple antennas are straightforward.

### A. Approximating the channel's impulse response

As shown in Fig. 2, we consider a wireless channel between two radio transceivers, referred to as user equipment (UE) and basestation (BS), which are both equipped with a single antenna. The channel impulse response  $h(\tau)$  can be written as

$$h(\tau) = \sum_{p=1}^P a_p \delta(\tau - \tau_p) \quad (1)$$

where  $a_p \in \mathbb{R}_+$  and  $\tau_p \in \mathbb{R}_+$  for  $p = 1, \dots, P$  are the attenuation and propagation delay of the  $p$ th path, respectively. The channel impulse response is reciprocal, i.e., it characterizes the channel between both transceivers in each directions. Both transceivers communicate using an FDD scheme, where one frequency band is used for UL transmissions from the UE to the BS, while another frequency band is used for DL transmissions from the BS to the UE. Both frequency bands are of bandwidth  $W$  and have center frequencies  $f_{\text{UL}}$  and  $f_{\text{DL}}$ , respectively. In the following we assume that (1) is valid over a large frequency range  $[\min(f_{\text{UL}}, f_{\text{DL}}) - W/2, \max(f_{\text{UL}}, f_{\text{DL}}) + W/2]$ , sufficient to contain both the UL and DL frequency bands.

Following [21], the equivalent discrete time baseband model of the channel  $h(\tau)$  over a frequency band of bandwidth  $W$  and center frequency  $f_c$  is given as

$$h_\ell = \sum_{p=1}^P a_p e^{-j2\pi f_c \tau_p} \text{sinc}(\ell - \tau_p W) \quad \ell = 0, \dots, L-1 \quad (2)$$

where  $\text{sinc}(x) = \frac{\sin(\pi x)}{\pi x}$  is the normalized sinc-function and  $L$  is the largest integer for which  $|h_L| \geq \varepsilon$ , for some threshold  $\varepsilon > 0$ . Evaluating (2) for  $f_c = f_{\text{UL}}$  and  $f_c = f_{\text{DL}}$ , we obtain the equivalent discrete time baseband UL and DL channels  $h_{\ell, \text{UL}} \in \mathbb{C}$  and  $h_{\ell, \text{DL}} \in \mathbb{C}$ , respectively.

Due to the finite sampling rate  $W$ , it is generally impossible to estimate the exact values of  $\tau_p$  from  $h_{\ell, \text{UL}}$  or  $h_{\ell, \text{DL}}$  for any arbitrary  $f_{\text{UL}}$  to  $f_{\text{DL}}$ , e.g., from 1 GHz to 6 GHz. It is, therefore, also impossible to compute the exact values of  $h_{\ell, \text{DL}}$  from  $h_{\ell, \text{UL}}$  and vice versa. However, a NN can predict an *approximation* of  $h_{\ell, \text{DL}}$  from  $h_{\ell, \text{UL}}$  (or vice versa) for a given radio environment at an adjacent frequency band.

We denote by  $\mathbf{h}_{\text{UL}} \in \mathbb{C}^{N_{\text{sub}}}$  and  $\mathbf{h}_{\text{DL}} \in \mathbb{C}^{N_{\text{sub}}}$  the CSI vectors over subcarriers of an OFDM system.

### B. Metrics

Throughout this work, three different performance metrics are used, each of which coming with its own strengths and weaknesses, as will be discussed next.

1) *Normalized mean squared error (NMSE)*: We use the NMSE as the loss function during training given as

$$\text{NMSE} = \mathbb{E} \left[ \frac{\|\mathbf{h}_{\text{DL}} - \hat{\mathbf{h}}_{\text{DL}}\|_2^2}{\|\mathbf{h}_{\text{DL}}\|_2^2} \right]. \quad (3)$$

While the mean squared error (MSE) is a standard metric for regression tasks, our task requires a normalization such that the performance is independent of the path loss, i.e.,  $\mathbb{E} [|\mathbf{h}_{\text{DL}}|^2] = 1$ , which would otherwise suggest misleading results. The normalization forces the NN to also focus on channel coefficient characteristics for distant UE positions, where  $|\mathbf{h}_{\text{DL}}|^2$  is comparatively small. By only training on the MSE without normalization, the NN tends to learn to output a random near-zero prediction for input CSI where  $\mathbb{E} [|\mathbf{h}_{\text{UL}}|^2]$  is small. However, the drawback of the NMSE is that its interpretation is less intuitive in how the NMSE relates to the achieved performance and, thus, we, rather, consider the correlation coefficient for most evaluations.

2) *Correlation coefficient*: We use the *correlation coefficient*  $\delta_h$  as an alternative performance metric, allowing a more intuitive interpretation. The correlation coefficient is defined as

$$\delta_h = \mathbb{E} \left[ \frac{\|\mathbf{h}_{\text{DL}} \hat{\mathbf{h}}_{\text{DL}}^H\|_2}{\|\mathbf{h}_{\text{DL}}\|_2 \|\hat{\mathbf{h}}_{\text{DL}}\|_2} \right] = \mathbb{E} \left[ \frac{\sum_{k=0}^{N_{\text{sub}}} \|h_{k,\text{DL}} \hat{h}_{k,\text{DL}}\|_2}{\|\mathbf{h}_{\text{DL}}\|_2 \|\hat{\mathbf{h}}_{\text{DL}}\|_2} \right]. \quad (4)$$

Its main advantage is that it provides a very intuitive result, as the range is bounded by the perfect match between predicted and actual channel (i.e.,  $\delta_h = 1$ ) and an uncorrelated scenario (i.e.,  $\delta_h = 0$ ). Note that, a common phase rotation for all elements of the prediction does not affect this metric. However, a constant phase offset is inherently compensated by the underlying OFDM scheme. In our experiments we observed, in contrast to NMSE, that the correlation coefficient is not a suitable loss function. It converged quickly to a local minimum with unsatisfactory performance.

3) *Bit error rate (BER)*: Despite the fact that the NMSE and correlation coefficient provide good metrics for comparing the similarity of the predicted CSI, it does not tell us anything about the resulting BER performance. Thus, we also evaluate the (uncoded) BER when operating the system with the predicted channel coefficients. This means we precode/equalize quadrature phase shift keying (QPSK) symbols based on predicted CSI by the NN, and then evaluate on a channel that uses the actual CSI. While the BER metric also provides a good insight into the NN's performance, its drawback is that, unfortunately, it cannot be directly embedded as loss function, as it requires intensive Monte-Carlo simulations per prediction, and, moreover, is not differentiable. One could possibly use soft information, i.e., cross-entropy if needed.

### III. A PRIMER ON DEEP LEARNING AND DATASETS

We provide a brief introduction to deep learning with the aim of clarifying notation and terminology used throughout this work. However, we refer the interested reader to [22] for further details on deep learning in general.

A neural network (NN) consists of weights  $\boldsymbol{\theta}$ , within a certain layer structure, that define a mapping

$$\hat{f}(\mathbf{x}; \boldsymbol{\theta}) : \mathbb{R}^n \mapsto \mathbb{R}^k \quad (5)$$

of an input vector  $\mathbf{x} \in \mathbb{R}^n$  to an output vector  $\hat{\mathbf{y}} \in \mathbb{R}^k$ . The weights  $\boldsymbol{\theta}$  determine the NN's behavior, and the process of finding good values for  $\boldsymbol{\theta}$  from data to achieve a desired behavior is generally described as "deep learning". In our case the input vector  $\mathbf{x}$  is the CSI of one channel (subcarriers) at a frequency centered around  $f_{\text{UL}}$  and the desired behavior of the NN is to output a prediction  $\hat{\mathbf{y}}$  of the CSI of another channel at another frequency band centered around  $f_{\text{DL}}$ . This is called a regression task and we can use well-established algorithms to fit the weights to our datasets such that they minimize a certain loss metric. A single complex-valued number is split into two consecutive real-valued numbers and used as input for the NN and, vice versa, at the output.

We start training with small mini-batches containing only 16 samples and increase the batchsize during the process stepwise up to 512 to obtain more fine-grained weight updates. During training, we also add additive white Gaussian noise (AWGN) as regularization to the training samples to prevent overfitting.

Intuitively, the optimal training signal-to-noise-ratio (SNR) is a trade-off between high noise power, i.e., *learning robustness to noisy data* and noiseless samples, i.e., *learning the underlying (deterministic) channel transfer function* [23].

#### A. Dataset

We can easily generate large quantities of simulated or measured channel realizations on both frequency bands at  $f_{\text{UL}}$  and  $f_{\text{DL}}$ , respectively. Our datasets contain labeled samples, i.e., a sample is a tuple of input  $\mathbf{x} = \mathbf{h}_{\text{UL}}$  and label  $\mathbf{y} = \mathbf{h}_{\text{DL}}$ . Our

dataset contains  $N$  samples denoted by  $\{(\mathbf{h}_{UL,1}, \mathbf{h}_{DL,1}), \dots, (\mathbf{h}_{UL,N}, \mathbf{h}_{DL,N})\}$ . In all our simulations and measurements we use an OFDM scheme with  $N_{sub} = 1024$  subcarriers. Due to guard-bands, we effectively use 922 out of those 1024 subcarriers, resulting in a CSI vector of 922 complex channel coefficients. We reshape those coefficients to their real-valued real and imaginary parts and also use multiple antennas in the MIMO scenario. Thus, the dimensionality of both the input and the label tensor is  $M \times N_{sub} \times 2$  (nb. antennas, nb. subcarriers, real/imaginary part). All datasets are randomly split into a train set, containing 90%, and a test set, containing 10% of all samples.

### B. Convolutional Layers

Our final NN structure mainly consists of convolutional neural network (CNN) layers, reducing the total amount of trainable parameters by order of magnitudes. Since neighboring OFDM channel coefficients in frequency domain are correlated within the coherence bandwidth, we figured that convolutional layers are perfectly suited to extract latent information. Thus, we use multiple two-dimensional convolutional layers with different kernel sizes in our final NN structure, which is similar to established models in computer vision like VGG [24]. Furthermore, additional pooling layers after each CNN layer are used to reduce the dimensionality of the input tensor. As final output we use a dense layer with linear activation to create the channel coefficients of the DL in the desired output shape.

## IV. SISO UL-DL CHANNEL PREDICTION

We first focus on the SISO scenario to illustrate the differences between the previously described performance metrics, and show the viability of this concept. However, it is important to realize that a solution for the SISO scenario directly provides a *naive* MIMO solution (by applying  $M$  independent estimators).

### A. Basic Example: line-of-sight (LoS) Model

If we consider a pure LoS scenario with distance dependent pathloss, the UL and DL channel impulse responses for a distance  $d$  between both transceivers are given by

$$h_{UL}(d) = \left(\frac{c}{4\pi f_{UL} d}\right)^\beta e^{-j2\pi f_{UL} \frac{d}{c}} \quad (6)$$

$$h_{DL}(d) = \left(\frac{c}{4\pi f_{DL} d}\right)^\beta e^{-j2\pi f_{DL} \frac{d}{c}} \quad (7)$$

where  $\beta > 2$  is a pathloss exponent and  $c$  is the speed of light. In this scenario, we do not use OFDM channel coefficients, since there is only a single LoS path, resulting in a system which is already frequency flat. Therefore, we only consider one channel coefficient for each  $f_{UL}$  and  $f_{DL}$ , respectively. We also denote the UL/DL band separation as  $\Delta f = f_{DL} - f_{UL}$  in the following. Since the underlying channel function is known in this example, there are several approaches to tackle the task of estimating  $h_{DL}$  from  $h_{UL}$ .

1) *Classic analytical channel estimation*: It is apparent from (6) that the absolute value of  $|h_{UL}|$  is only dependent on  $d$ . Thus, the only difficulty is to predict the distance  $d$  of  $h_{UL}$  based on the magnitude of  $h_{UL}$ . Since  $d = \frac{c}{4\pi f_{UL} |h_{UL}(d)|^{1/\beta}}$ , we have

$$h_{DL}(d) = \left(\frac{f_{UL}}{f_{DL}}\right)^\beta |h_{UL}(d)| \exp\left(-j \frac{f_{DL}}{2f_{UL} |h_{UL}(d)|^{1/\beta}}\right). \quad (8)$$

This means that a NN only needs to learn a mapping of the form  $f(x) = xe^{-jK|x|^{-\frac{1}{\beta}}}$  (and the distance  $d$ ) from the observations, which is clearly possible provided that enough training samples  $\{(\mathbf{h}_{UL,1}, \mathbf{h}_{DL,1}), \dots, (\mathbf{h}_{UL,N}, \mathbf{h}_{DL,N})\}$  are available. Note that this approach only works as a baseline for the pure LoS scenario.

2) *Wiener filter estimation*: A classic approach to estimate CSI in time and frequency domain is the Wiener filter (also referred to as linear minimum mean square error (LMMSE) estimator) [25]. The Wiener filter coefficients are defined as

$$\mathbf{c}_{\text{LMMSE}} = (\mathbf{R}_{UL,UL} + \sigma^2 \mathbf{I})^{-1} \mathbb{E} [\mathbf{h}_{UL} \mathbf{h}_{DL}^H] \quad (9)$$

with noise variance  $\sigma^2$  (complex noise samples) and

$$\mathbf{R}_{UL,UL} = \mathbb{E} [\mathbf{h}_{UL} \mathbf{h}_{UL}^H]. \quad (10)$$

To estimate unknown CSI, we match the closest known validation  $\mathbf{h}_{UL}$  point to the current test point  $\mathbf{h}'_{UL}$  by using the correlation and by taking its filter coefficients  $\mathbf{c}'_{\text{LMMSE}}$  to estimate

$$\hat{\mathbf{h}}_{DL} = \mathbf{c}'_{\text{LMMSE}} \mathbf{h}'_{UL}. \quad (11)$$

3) *NN-prediction approach*: The fact that there exists a function (8) that analytically solves this toy case, the universal approximation theorem [26] tells us that there exists a NN that can approximate, or *learn*, this function arbitrary well. We therefore use a basic NN structure (shown in Table I) based on feed-forward dense layers to solve this task.

TABLE I: NN architecture for LoS experiments

Layers:	Trainable parameters	Output dimensions
Input	0	2 (Re/Im)
Dense	384	128
Dense	33,024	256
Dense	263,168	1024
Dense	26,400	256
Dense	32,896	128
Dense	258	2 (Re/Im)

The NN receives a single channel coefficient  $h_{UL}$  as input and predicts the corresponding single channel coefficient  $h_{DL}$  as output. We train this NN with samples created according to (6), where the UE is randomly positioned within a radius ranging from 100 m to 200 m around the BS. Also, the results are inferred on random positions within this range.

We evaluate all three aforementioned approaches with 5,000 randomly positioned samples (UEs) based on the LoS pathloss model (6) and test all approaches on predicting the correct  $h_{DL}$  from the given  $h_{UL}$ . Then, we take the previously described BER metric with predictions  $\hat{h}_{DL}$  to precode/equalize QPSK symbols transmitted over the actual channel characterized by  $h_{DL}$ .

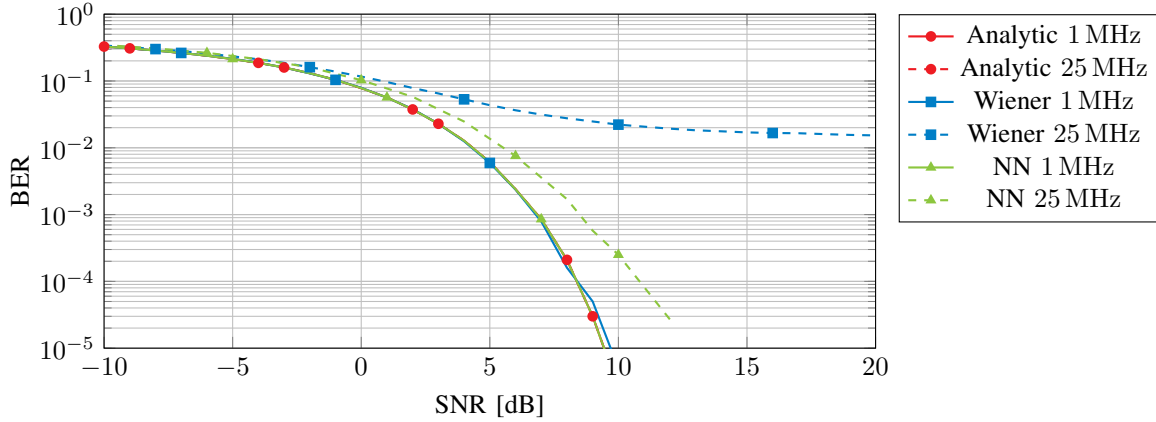


Fig. 3: BER curves of different estimation approaches in the LoS scenario; the NN is trained with 4,500 samples.

Fig 3 shows the results for a UL/DL band separation of  $\Delta f = f_{DL} - f_{UL} = 1$  MHz and  $\Delta f = 25$  MHz, respectively. As expected, the analytical solution leads to optimal results, hence coincides with the uncoded QPSK BER curve (the same holds for the Wiener filter at  $\Delta f = 1$  MHz). However, the more interesting observation is that the Wiener filter only works well for  $\Delta f = 1$  MHz, but not for  $\Delta f = 25$  MHz. Intuitively, this can be explained by the fact that the Wiener filter needs to extrapolate the DL CSI from only one specific UL CSI sample depending on the actual position. The autocorrelation matrix does not contain the spatial dependencies and, thus, the classical Wiener filter approach *fails* for most tasks. Unfortunately, to the best of our knowledge, this is the best estimator for extrapolation in frequency domain (without any further channel sparsity assumption). The NN, on the other hand, achieves optimal results for  $\Delta f = 1$  MHz, however, shows some degradation for  $\Delta f = 25$  MHz. This degradation can easily be reduced by supplying more training samples. By limiting the amount of training samples to only 4,500 for both the  $\Delta f = 1$  MHz separation and the  $\Delta f = 25$  MHz separation, we can see that predictions on a close-by frequency band ( $\Delta f = 1$  MHz) are *easier* for the NN. We also achieved optimal prediction results for  $\Delta f = 25$  MHz in this simple LoS toy case scenario after training the NN with  $\geq 10,000$  samples. Contrary to the analytical solution, the NN approach is completely independent of knowing the underlying channel model, whereas the analytical solution only works for this simple LoS model.

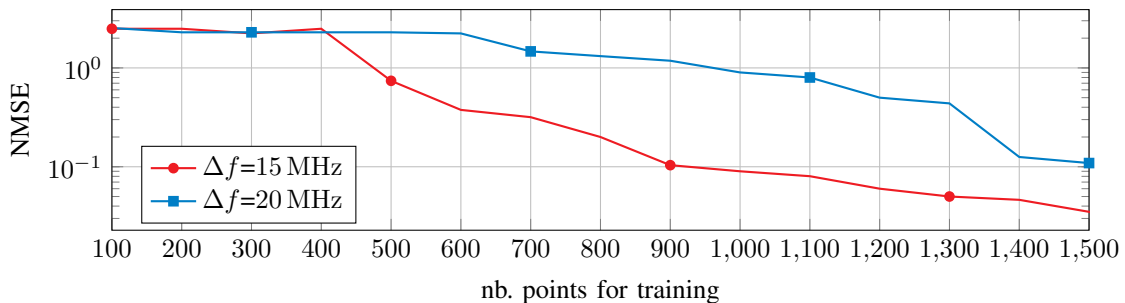


Fig. 4: NMSE versus number of training points and different frequency band separations  $\Delta f$ .

Fig. 4 shows the influence of different amounts of training samples for  $\Delta f = 15$  MHz and  $\Delta f = 25$  MHz, respectively. It takes about 400 to 600 different samples during training for the NN to start to generalize. Obviously, a larger frequency band separation  $\Delta f$  between UL and DL also requires a higher number of training samples to sufficiently solve the task, as the relation between input and label appears to be more *random* from the NNs's point-of-view. Intuitively, this can be explained due to periodicity of the phase rotation in (6), causing the same input phase to be projected onto more than one



output phase. Therefore, the single most relevant variable, that is, the amplitude, needs to be estimated more precisely for larger band separation  $\Delta f$ .

### B. Simulated Results: Standardized Channel Models

Next, we evaluate NN-based channel prediction in a more realistic setting using standardized channel models provided by the Quadriga framework [20], such as the *Winner II*, *3GPP* and *Berlin* model.

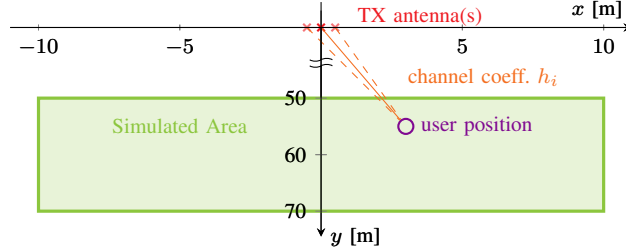


Fig. 5: Spatial simulation area for different channel models.

The simulation setup is depicted in Fig. 5. We use the channel models to simulate the CSI at  $f_{UL}$  and  $f_{DL}$  between a fixed BS and a UE at random spatial positions within the same environment. An area of  $400m^2$  is simulated with an average distance per spatial UE position of  $\sim 12.5cm$  resulting in 22,500 samples. Per UE position, we estimate the channel for two different frequency band separations ( $\Delta f = 25$  MHz,  $\Delta f = 50$  MHz) between  $f_{UL}$  and  $f_{DL}$ . For this, we use an OFDM system with 1024 subcarriers and a cyclic prefix (CP) length of 256 symbols with two dipole antennas at frequency bands centered around 1.25 GHz and 1.275 GHz (1.3 GHz for  $\Delta f = 50$  MHz, respectively) with a bandwidth of  $B = 20$  MHz for both the UL and DL frequency band.

Note that it is necessary to enable Quadriga’s *spatial consistency* parameter to ensure that the simulation environment, i.e., positions of scatterers, does not change when the UE changes its position. Random realizations of different environments would render the channel prediction task impossible, as the NN would not be able to learn an underlying physical channel scattering behavior. For all SISO results, the antenna geometry does not need to be considered and, thus, we only use 1-D convolutional layers in our NNs. The hyperparameters of this SISO NN structure, as described in Tab. II, was trained at an  $SNR = \|\mathbf{h}\|_2^2 / 2\sigma^2$  of 10 dB, where  $\sigma^2$  is the noise variance.

TABLE II: NN architecture for SISO experiments

Layers:	Trainable parameters	Output dimensions
Input	0	1024 x 2 (Re/Im)
Conv1D	416	1024 x 32
Average Pooling	0	256 x 32
Conv1D	3088	256 x 16
Average Pooling	0	64 x 16
Flatten	0	1024
Dense	131,200	128
Dense	16,512	128
Dense	16,512	128
Dense	264,192	2048
Reshape	0	1024 x 2 (Re/Im)

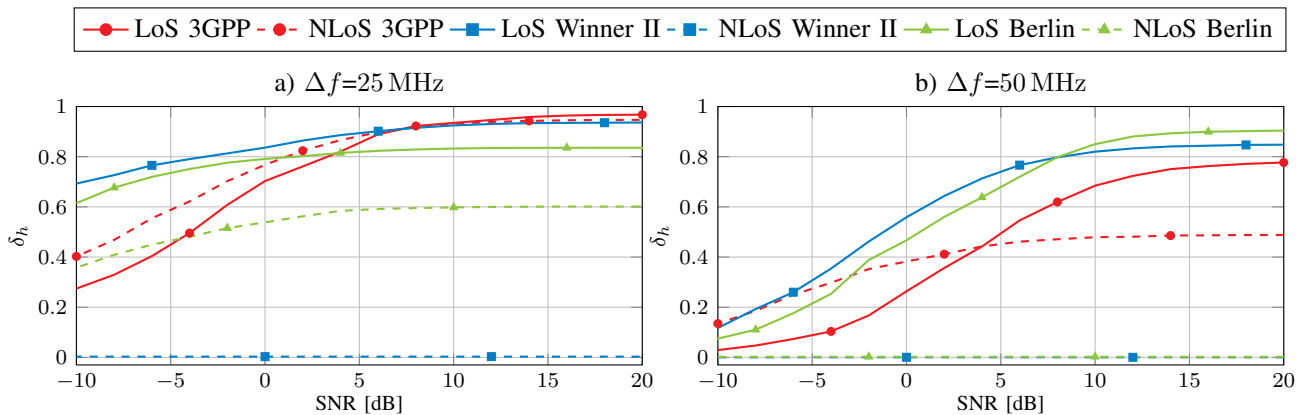


Fig. 6: NN-based CSI-prediction: correlation coefficient versus SNR with different SISO channel models at band separations  $\Delta f = 25$  MHz (a) and  $\Delta f = 50$  MHz (b).

Fig. 6 shows the correlation coefficient  $\delta_h$  for a frequency band separation of  $\Delta f = 25$  MHz (left) and  $\Delta f = 50$  MHz (right) between the UL and DL versus the SNR. As can be seen, the NN estimator (see Table II) is able to predict the CSI for these standardized channel models, and the NN can generalize over a wide range of different SNRs. In the LoS scenario, all three different channel models lead to a reasonable performance ( $\delta_h \geq 0.8$ ) by the NN. Simulations on spectral efficiency (shown later in Section V) indicate that a correlation coefficient of  $\delta_h = 0.8$  results in an maximum ratio transmission (MRT) sum-rate performance loss of less than 10%. For the 3GPP model, the NNs performance is very similar for both the LoS and NLoS scenario in terms of the correlation metric. Although the performance is worse for the NLoS scenario with the *Berlin* model, a generalization of the NN can still be observed, resulting in a correlation coefficient of  $\delta_h \sim 0.6$ . The prediction does not work at all for the NLoS scenario with the *Winner II* model. As already mentioned concerning the *spatial consistency* parameter, the variations among the results of the three models can be explained by the differences between the channel models themselves:

- The 3GPP model uses consistency in both the spatial domain and the frequency domain in accordance to 3GPP 38.901 v14.1.0. Therefore, the NN can predict between close frequencies.
- Since the Winner II model is not based on this feature [20], the NN can only learn the environment in a more or less frequency flat scenario (LoS).
- Although the NLoS Berlin model is based on measurements (from which parameters were extracted, which were then used to re-simulate the measurement results) the model relies mainly on statistics rather than on actual environments (scatterers). Thus, an underlying frequency dependency does probably not exist in this model.

As expected, when the frequency band separation increases to  $\Delta f = 50$  MHz, the correlation coefficient decreases. Although the NN-based prediction still works in the LoS scenarios, no meaningful prediction can be provided for the NLoS scenario due to a weaker frequency dependency between UL and DL. However, a larger training dataset may further improve the performance. Note again that the Wiener filter-based approach fails for all investigated scenarios.

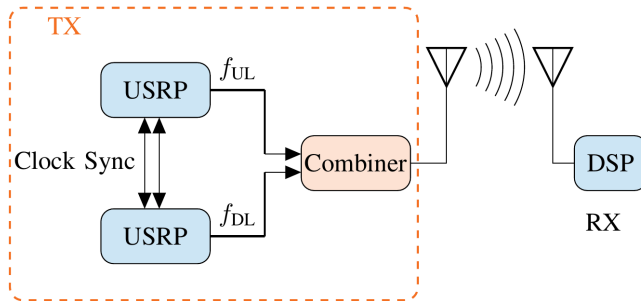


Fig. 8: Setup for the SISO link measurement.

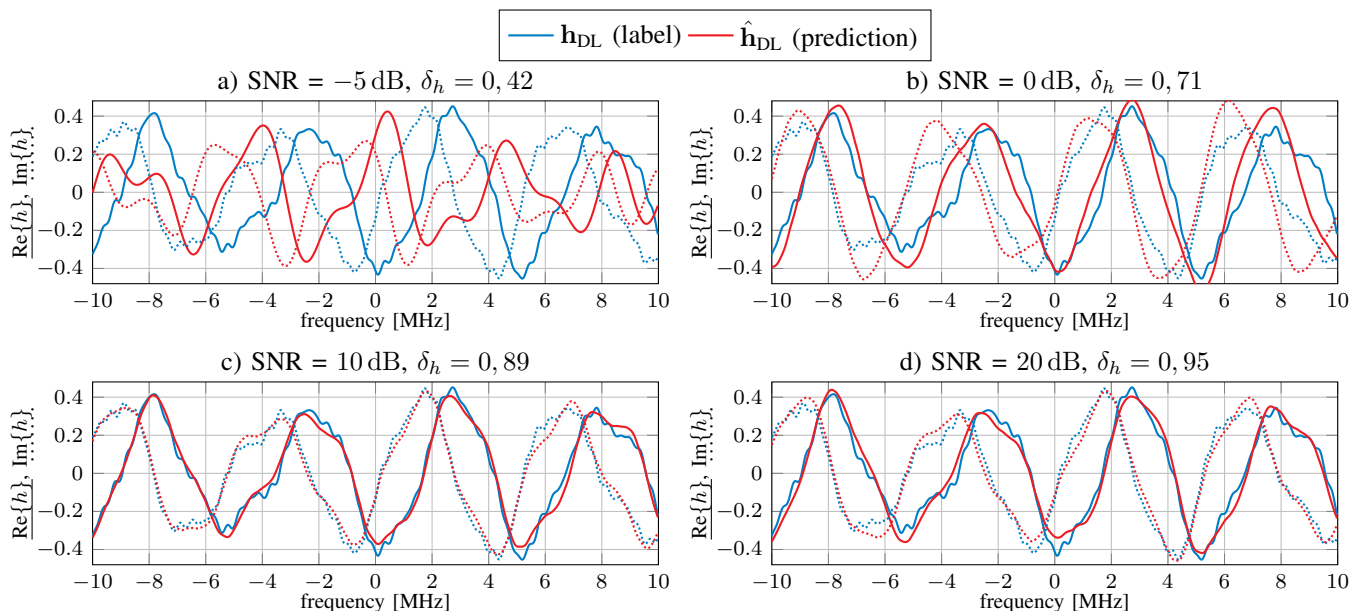


Fig. 7: Illustration of NN-based channel prediction for varying SNRs, 3GPP 38.901 LoS channel model.

To better illustrate the impact of the correlation coefficient, Fig. 7 shows a visualization of the prediction outcome and the corresponding ground truth for the 3GPP 38.901 model versus different SNR, while the NN was trained at SNR = 10 dB. Note that the channel can be accurately predicted between UL and DL frequency bands for positive values of the SNR (in dB). Thus, as a first major result of this paper, we show that the proposed NN architecture can predict the DL CSI for the SISO scenario.<sup>2</sup>

### C. Measurement data: SISO

Although the previously introduced channel models provide quite realistic test cases, and their properties have been verified through measurements by multiple independent research groups, the question whether DL channel prediction works on *actually measured* channels still remains open. One should keep in mind that most channel models are built for system performance evaluation where exact position-dependent precision is typically unnecessary. Further, we expect many hardware impairments in a practical system, which are difficult to cover in model-based approaches. To address these issues, we evaluate the NN prediction performance on measured channels, as described next.

<sup>2</sup>We want to emphasize that such a SISO result directly enables naive MIMO implementation by using  $M$  independent estimators.

To measure any combination of UL and DL frequencies, two universal software radio peripherals (USRPs) (B200 + B210) [27] are synchronized and combined on a single antenna as shown in Fig. 8. A single antenna is needed to ensure the exact same distance  $d$  between the transceivers. Typically, FDD systems also use the same antenna (in this case a horizontally polarized dipole) for UL and DL transmissions. The USRPs transmit at 1.25 GHz, 1.275 GHz and 1.3 GHz, respectively, with 20 MHz bandwidth each. The radio signal is transmitted over the channel, received with the horizontally polarized dipole antenna and then sampled at the carrier frequency by a wideband digital oscilloscope. UL and DL transmissions are then separated by an offline signal processing step (filtering). An extension to multiple (MIMO) receiver antennas is straightforward (see [28, daughterboard concept]).

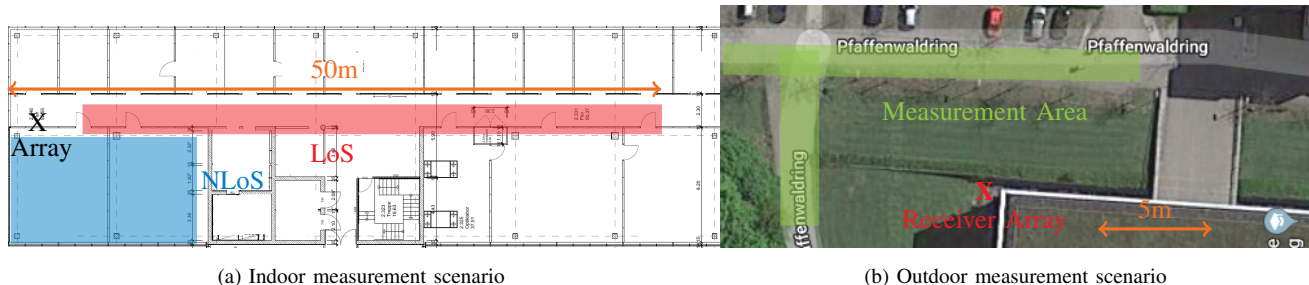


Fig. 9: Measurement scenarios: a) indoor b) outdoor.

To evaluate the performance in different scenarios, we distinguish between indoor and outdoor environments (see Fig. 9). Note that, the same scenarios are also used for the MIMO setup later in Section V. The indoor measurements include an LoS environment, consisting of our institute’s hallway, and an NLoS environment, represented by typical office space. Both indoor measurements were conducted within a static environment (at night), i.e., the environment did not change significantly during the measurements. The covered area is about  $200\text{ m}^2$  in the LoS scenario and about  $80\text{ m}^2$  in the NLoS scenario. For the outdoor measurement, a typical Rician fading scenario can be expected, in a campus environment with tall buildings surrounding the measured area of about  $250\text{ m}^2$ . We acquired 4,000 measurement samples per scenario. All positions were measured in a meander-like path, however, the samples were randomly permuted during training, i.e., training and validation data were randomly selected from the entire area (90% training and 10% validation).

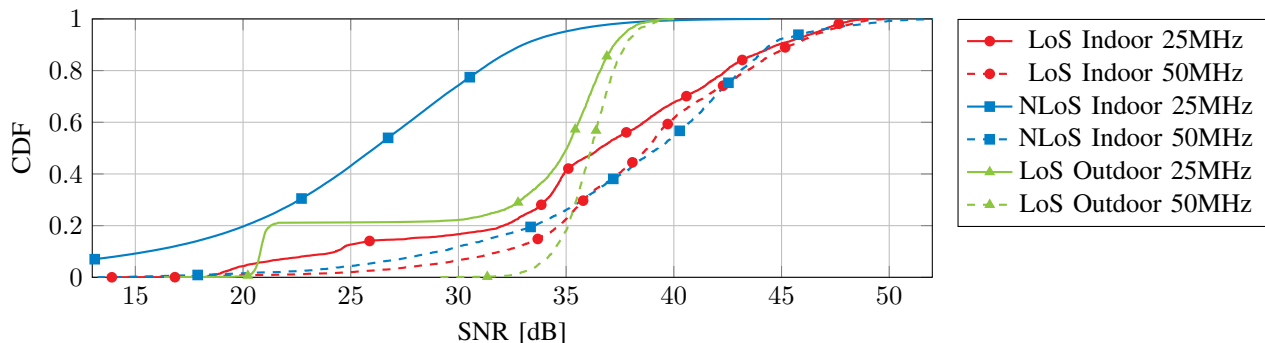


Fig. 10: CDF of the received SNR for different measurement scenarios.

To verify the measurement data, Fig. 10 depicts the acquired channel quality. The SNR, calculated using the error vector magnitude (EVM) for all measurements, is around 20 dB and, thus, accurate channel predictions are possible. The different noise figures are caused by the two different USRP devices.

TABLE III: Results of SISO channel prediction for measured data

$\Delta f$	Indoor LoS	Indoor NLoS	Outdoor LoS
25 MHz	$\delta_h=0.95$	$\delta_h=0.80$	$\delta_h=0.93$
	NMSE=-20 dB	NMSE=-17 dB	NMSE=-23 dB
50 MHz	$\delta_h=0.90$	$\delta_h=0.77$	$\delta_h=0.87$
	NMSE=-19 dB	NMSE=-14 dB	NMSE=-21 dB

The results, in Table III, show that the NN achieves reasonable precision for all scenarios studied. As expected the indoor NLoS scenario is worse when compared to the corresponding LoS scenario, but, still, in a reasonable range. One must keep in mind that these results are based on actual measurements including several impairments, e.g., caused by hardware tolerances and quantization effects. Thus, the used labels (i.e., measured CSI) are already compromised by noise and distortion stemming from an imperfect (but unavoidable) measurement setup. Again, the prediction quality in all three environments turns out to be sufficiently good, suggesting deployment of the proposed system in a real world physical channel in the SISO context.

## V. MIMO UL-DL CHANNEL PREDICTION

Next, we consider the practically more relevant MIMO scenario, i.e., we assume multiple antennas at the BS and try to enable FDD Massive MIMO, without the need of imposing any sparsity constraint on the channel. Although multiple trained SISO estimators can be stacked to build such a MIMO system, we want to study whether true MIMO signal processing (i.e., exploration of correlations between antennas) can further improve prediction accuracy.

### A. System Model

We consider a single-antenna UE and a BS equipped with  $M$  antennas. We denote the UL and DL channels from the UE to the  $m$ -th antenna of the BS by  $\mathbf{h}_{\text{UL}}^{(m)} \in \mathbb{C}^{N_{\text{sub}}}$  and  $\mathbf{h}_{\text{DL}}^{(m)} \in \mathbb{C}^{N_{\text{sub}}}$ , for  $m = 1, \dots, M$ , respectively. The investigations of Section IV are extended to the MIMO system model in the following.

### B. Simulated LoS Model

Similar to Section IV-A, we first investigate the performance of a simple LoS Massive MIMO system. To verify whether the channel prediction limits the gain of the linear precoding scheme, the classic MRT is investigated. The received signal per subcarrier  $k$  is defined as

$$y_k = \mathbf{h}_k \mathbf{w}_k^H s_k + \mathbf{n}_k \quad (12)$$

where  $\mathbf{w}_k$  is the  $1 \times M$  linear precoding vector,  $\mathbf{h}_k$  is the  $1 \times M$  channel vector,  $s_k$  is the transmitted QPSK symbol and  $\mathbf{n}_k$  is the  $1 \times 1$  additive white Gaussian noise vector. The linear precoder for MRT is defined as

$$\mathbf{w}_k = \frac{\hat{\mathbf{h}}_k}{\|\hat{\mathbf{h}}_k\|_2}. \quad (13)$$

We use the same settings as in Section IV with  $\Delta f = 25$  MHz and a NN as depicted in Table I (extended to the current number of antennas  $M$ ). We observe a growing training complexity, yet the required amount of data points does not increase with the number of antennas. Intuitively, this can be explained by the fact, that (per antenna) the problem itself has similar complexity as in the SISO scenario. However, due to the increased input dimensions, the task of finding an underlying structure from observations becomes more complex for larger input dimension (*more randomness* in the input).

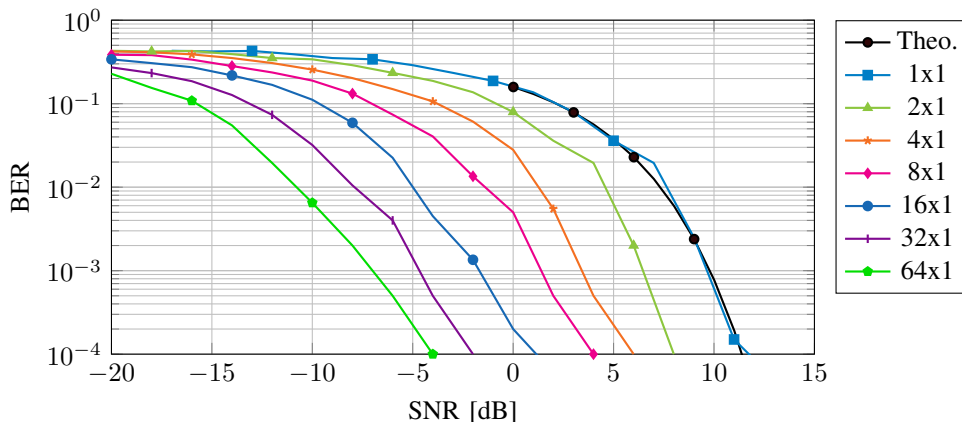


Fig. 11: NN-based CSI prediction: BER curves for LoS MIMO.

The BER curves in Fig. 11 show the expected 3 dB gain whenever the number of antennas is doubled. Also, the analytical BER curve matches with the simulated  $1 \times 1$  curve. Unfortunately, the joint prediction does not seem to improve performance (same NMSE per antenna as in the SISO scenario), indicating that the NN does not benefit from multiple antennas (only from MRT). This could be explained by the fact that the antennas are assumed to be uncorrelated and, thus, each antenna needs to be predicted by itself, as the positions are also uncorrelated.

### C. Results for standardized MIMO channel models

We now extend our NN model as given in Table IV to the MIMO input. A rectangular  $8 \times 8$  patch antenna array is used for all simulated scenarios ( $8 \times 4$  for the measurement scenarios) and the UL/DL band separation is  $\Delta f = 25$  MHz.

TABLE IV: NN architecture for MIMO experiments

Layers:	Output dimensions
Input	$M \times 1024 \times 2$ (Re/Im)
Conv1D	$1024 \times 32$
Average Pooling	$256 \times 32$
Conv1D	$256 \times 16$
Average Pooling	$64 \times 16$
Flatten	1024
Dense	16
Dense	32
Dense	64
Dense	$M \cdot 2048$
Reshape	$M \times 1024 \times 2$ (Re/Im)

Obviously, the amount of trainable parameters increases from  $\sim 400,000$  weights to approximately 8 million weights caused by the increased input dimensionality ( $M$  antennas instead of 1). However, somewhat to our surprise, experiments conducted with 2-D CNN structures did not yield a significant improvement in prediction performance (occasionally even slightly worse). One potential explanation is that, with an increased number of antennas, the environment complexity also increases, as the number of scatterers can be different.

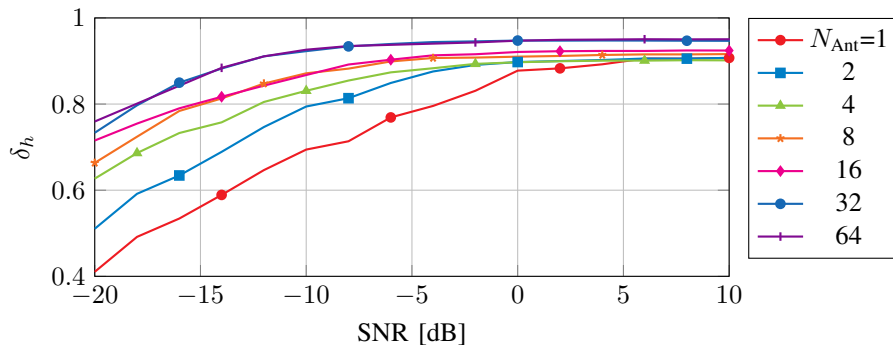


Fig. 12: NN-based CSI-prediction: correlation coefficient versus SNR with different number of antennas in 3GPP LoS.

The influence of different numbers of antennas on the correlation coefficient is depicted in Fig. 12 for the 3GPP LoS scenario; the training SNR was fixed to 10 dB. It can be seen that the correlation coefficient for higher SNR only changes slightly, but the system becomes more robust against noise with an increasing number of antennas. Note that, due to the way we select the antennas from our dataset (without changing the aperture size), the results for 64/32 and 16/8 are similar.

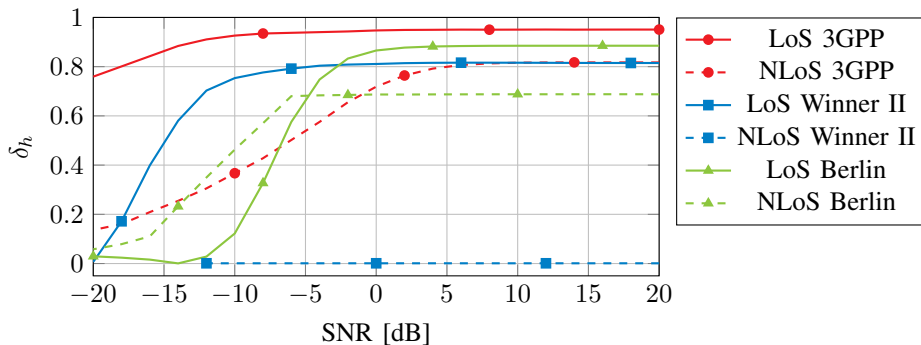


Fig. 13: NN-based CSI-prediction: correlation coefficient versus SNR with different MIMO channels using 64 antennas.

Fig. 13 shows the correlation coefficient over SNR for different Massive MIMO channel models. As can be seen, the prediction performance is comparable to the performance achieved in the SISO scenario. The prediction accuracy for the 3GPP model is within a reasonable region as the previously described margin of a correlation coefficient of  $\delta_h = 0.8$  is reached. Moreover, the predictions for the NLoS “Berlin” scenario show a better performance than their SISO counterparts, as, potentially, antennas correlations could be exploited.

We note the second major result of this paper: The proposed NN architecture can predict the DL CSI for the MIMO scenario with a UL/DL band separation of  $\Delta f = 25$  MHz (without requiring sparsity) and, therefore, enables FDD Massive MIMO for a wide range of different channels.

#### D. Results for actually measured MIMO channels

To further illustrate the scheme’s robustness against hardware impairments, we use the same measurement scenarios as in Section IV-C, but now for the MIMO case. The *subband* approach, introduced in [28], allows us to measure “Massive” MIMO with 32 Antennas arranged in a  $8 \times 4$  patch array configuration.

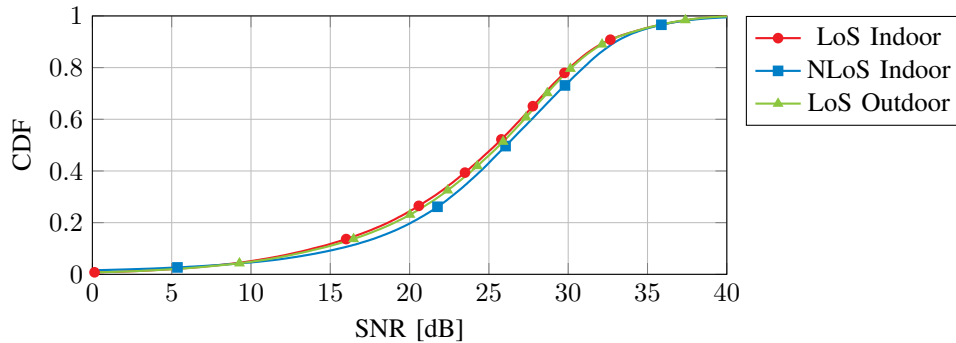


Fig. 14: CDF of the SNR for different measurement scenarios.

Fig. 14 shows the CDF of the SNR for all antennas, and for all three measurement scenarios, respectively. The SNR is, on average, around 25 dB resulting in useful datasets of around 5,000 spatial points per scenario. To evaluate the NN's prediction performance for this practical system we investigate the spectral efficiency by using different precoding schemes and numbers of users  $N_{\text{Users}}$ . The received signal signal of all UEs on the  $k$ th subcarrier is given by

$$\mathbf{y}_{k,\text{RX}} = \mathbf{H}_k \frac{\mathbf{W}_k}{\|\mathbf{W}_k\|_F} \mathbf{x}_k + \mathbf{n}_k \quad (14)$$

where  $\mathbf{x}_k$  is the  $N_{\text{Users}} \times 1$  transmit vector at subcarrier  $k$ ,  $\mathbf{H}_k$  is the  $N_{\text{Users}} \times M$  channel matrix stacked with the channel vectors  $\mathbf{h}_{k,1..N_{\text{Users}}}$ ,  $\mathbf{W}_k$  is the  $M \times N_{\text{Users}}$  precoding matrix,  $\mathbf{n}_k$  is the  $N_{\text{Users}} \times 1$  complex gaussian noise vector, and  $\mathbf{y}_{\text{RX}}$  is the  $N_{\text{Users}} \times 1$  receive vector. We precode on  $N_{\text{Users}}$  randomly picked UE positions of the dataset, with maximum ratio transmission (MRT)

$$\mathbf{W}_{k,\text{MR}} = \hat{\mathbf{H}}_k^H \quad (15)$$

and, alternatively, zero forcing (ZF) precoding

$$\mathbf{W}_{k,\text{ZF}} = \hat{\mathbf{H}}_k^H \left( \hat{\mathbf{H}}_k \hat{\mathbf{H}}_k^H \right)^{-1} \quad (16)$$

respectively. With this definition, the signal-to-interference-noise-ratio (SINR) per user  $u$  can be computed as

$$\text{SINR}_k(u) = \frac{\|\mathbf{h}_{k,u} \mathbf{w}_{k,u}\|_2^2}{\sum_{j=1, j \neq u}^{N_{\text{Users}}} \|\mathbf{h}_{k,u} \mathbf{w}_{k,j}\|_2^2 + \sigma^2}. \quad (17)$$

where  $\text{SINR}_k(u)$  is the SINR per user  $u$ . The effective sum-rate is then calculated as

$$R = \frac{1}{N_{\text{sub}}} \sum_{k=0}^{N_{\text{sub}}-1} \sum_{u=1}^{N_{\text{Users}}} \log_2(1 + \text{SINR}_k(u)). \quad (18)$$



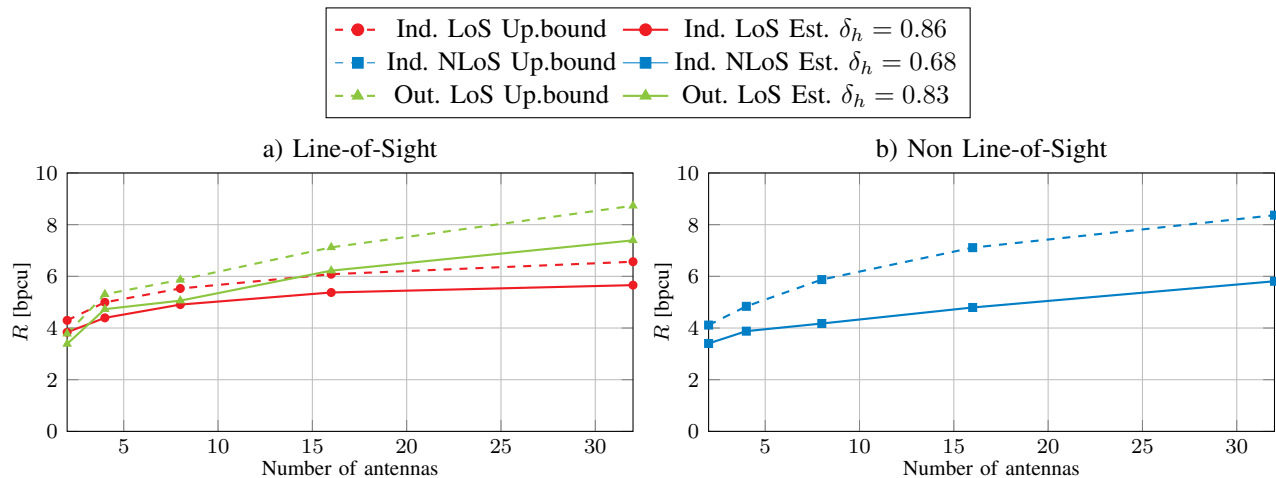


Fig. 15: Simulated sum-rate versus number of antennas for the measured LoS and NLoS scenarios in the case of MRT on two users; no DL pilots used.

The effective sum-rate based on the NN's predictions is given for all three scenarios in Fig. 15. We precode on two users with MRT and try to separate them. Note that the presented upper bound is based on the measured CSI of the DL frequency band, i.e., includes all hardware impairments plus noise (SNR=10 dB). It is, thus, not achievable with a genuine TDD system, even if we assume perfectly reciprocal hardware. Observe that the sum-rate based on our NN's predictions is only slightly worse ( $\leq 10\%$ ) than the TDD-bound in both LoS scenarios, and is still acceptable ( $\leq 20\%$ ) in the NLoS scenario, reaffirming that the NN-based system is a viable solution to enable FDD Massive MIMO. Furthermore it is a notable advantage that non-reciprocal hardware chains, like the one we used for these measurements, will directly be learned by our proposed NN-based prediction system. This means that reasonable spectral efficiency can be reached without perfectly reciprocal hardware.

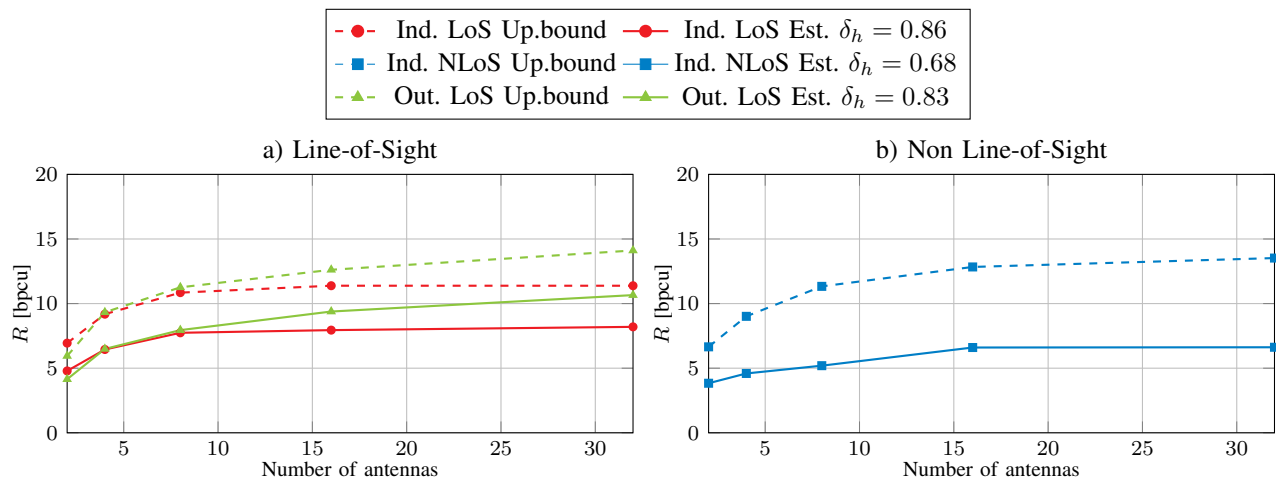


Fig. 16: Simulated sum-rate versus number of antennas for the measured LoS and NLoS scenarios in the case of ZF precoding on two users; no DL pilots used.

Fig. 16 provides results for the stricter case of ZF precoding on two users with an SNR of 10 dB. Since ZF precoding tries to orthogonalize the users by forcing the interference to zero, a slight mismatch does have a more dramatic effect than in the simpler case of MRT. As can be seen, the ZF sum-rate based on the NN's predictions is, again, only slightly worse ( $\leq 20\%$ ) than the TDD upper bound in both LoS scenarios, and is still working ( $\leq 45\%$  worse) in the NLoS scenario. There are several further improvements to the system at hand that may be considered in the future: a recurrent NN could be used,

an investigation into the sample density could be done, hyperparameter tuning of the NN should be considered and a revision of the measurement setup could provide cleaner training data at even higher SNR. Moreover, including the covariance matrix as expert knowledge could further improve the system performance.

## VI. CONCLUSION AND OUTLOOK

We introduced a NN-based scheme for extrapolating DL CSI from observed UL CSI in both SISO and MIMO scenarios, using simulated as well as actually measured channels. The new scheme outperforms the classic Wiener filter-based approach, and, even more so, allows to operate the system in cases where the Wiener filter would fail. Quantitatively, the NN-based channel prediction method leads to a spectral efficiency loss of only  $\sim 15\%$  in a two-user MRT setting when compared to a TDD-based system that is (unrealistically) assumed to be *perfect* in terms of hardware reciprocity and, thus, DL channel estimation. Obviously, it is key to have a large training dataset available and, by its very nature, additional retraining may be required whenever the radio environment changes significantly. It remains open for future research to further improve the NN architecture, e.g., by using recurrent NNs, by investigating the required sample density, by applying a Kalman filter to tackle time correlation, or by adding covariance matrix knowledge to the system. To facilitate follow-up studies, all channel measurements as well as all simulated data will be made publicly available so that results can be reproduced and improved as research in this practically highly relevant topic further progresses<sup>3</sup>.

## REFERENCES

- [1] E. Björnson, J. Hoydis, L. Sanguinetti, *Massive MIMO Networks: Spectral, Energy, and Hardware Efficiency*. now publishers, Nov. 2017.
- [2] J. Hoydis, S. ten Brink, M. Debbah, “Massive MIMO in the UL/DL of Cellular Networks: How Many Antennas Do We Need?” *IEEE Journal on Selected Areas in Communications*, pp. 160 – 171, Jan. 2013.
- [3] E. G. Larsson, O. Edfors, F. Tufvesson and T. L. Marzetta, “Massive MIMO for next generation wireless systems,” *IEEE Communications Magazine*, pp. 186 – 195, Feb. 2014.
- [4] F. Boccardi and R. W. Heath and A. Lozano and T. L. Marzetta and P. Popovski, “Five disruptive technology directions for 5G,” *IEEE Communications Magazine*, pp. 74 – 80, Feb. 2014.
- [5] R. S. Ganesan and W. Zirwas and B. Panzner and K. I. Pedersen and K. Valkealahti, “Integrating 3D Channel Model and Grid of Beams for 5G mMIMO System Level Simulations,” in *Vehicular Technology Conference*, Sept. 2016, pp. 1–6.
- [6] L. Miretti and L. G. Cavalcante and S. Stanczak, “FDD massive MIMO channel spatial covariance conversion using projection methods,” *IEEE International Conference on Acoustics, Speech and Signal Processing*, April 2018.
- [7] J. Nam and J. Ahn and A. Adhikary and G. Caire, “Joint spatial division and multiplexing: Realizing massive MIMO gains with limited channel state information,” in *46th Annual Conference on Information Sciences and Systems (CISS)*, March 2012, pp. 1–6.
- [8] E. Björnson, J. Hoydis, L. Sanguinetti, “Massive MIMO Has Unlimited Capacity,” *IEEE Transactions on Wireless Communications*, pp. 574 – 590, Nov. 2017.
- [9] E. Björnson, E. G. Larsson, and T. L. Marzetta, “Massive MIMO: Ten Myths and One Critical Question,” *IEEE Communications Magazine*, pp. 114 – 123, Feb. 2016.
- [10] Z. Gao and L. Dai and S. Han and C. I and Z. Wang and L. Hanzo, “Compressive Sensing Techniques for Next-Generation Wireless Communications,” *IEEE Wireless Communications*, pp. 144 – 153, Feb. 2018.
- [11] Z. Jiang and A. F. Molisch and G. Caire and Z. Niu, “On the achievable rates of FDD massive MIMO systems with spatial channel correlation,” in *International Conference on Communications in China (ICCC)*, Jan. 2015, pp. 276–280.
- [12] D. Vasisth, S. Kumar, H. Rahul, D. Katabi, “Eliminating Channel Feedback in Next-Generation Cellular Networks,” in *Special Interest Group on Data Communication (SIGCOMM)*, Aug. 2016, pp. 1–6.
- [13] W. Yang, L. Chen and Y. Liu, “Super-resolution for Achieving Frequency Division Duplex (FDD) Channel Reciprocity,” in *19th IEEE International Workshop on Signal Processing Advances in Wireless Communications*, Dec. 2018.
- [14] M. Soltani, A. Mirzaei, V. Pourahmadi and H. Sheikhzadeh, “Deep Learning-Based Channel Estimation,” *IEEE Communication Letters*, Oct. 2018.

<sup>3</sup>link available after review

- [15] H. Ye, G. Ye Li, B. Juang, "Power of Deep Learning for Channel Estimation and Signal Detection in OFDM Systems," *IEEE Wireless Communications Letters*, 2018.
- [16] Z. Jiang, Z. He, S. Chen, A. F. Molisch, "Inferring Remote Channel State Information: Cramer-Rao Lower Bound and Deep Learning Implementation," in *Globecom*, Dec. 2018.
- [17] R. Deng, Z. Jiang, S. Zhou, S. Cui, and Z. Niu, "A Two-Step Learning and Interpolation Method for Location-based Channel Database Construction," in *Globecom*, Dec. 2018.
- [18] P. Dong, H. Zhang and G. Ye Li, "Machine Learning Prediction based CSI Acquisition for FDD Massive MIMO Downlink," in *Globecom*, Dec. 2018.
- [19] M. Lorenzo and R. Cavalcante, and S. Stanczak, "Downlink channel spatial covariance estimation in realistic FDD massive MIMO systems," *IEEE Transactions on Wireless Communications*, pp. 574 – 590, April 2018.
- [20] S. Jaeckel, L. Raschkowski, K. Börner, and L. Thiele, "QuaDRiGa: A 3-D multi-cell channel model with time evolution for enabling virtual field trials," *IEEE Trans. Antennas Propag.*, pp. 3242 – 3256, 2014.
- [21] D. Tse and P. Viswanath, *Fundamentals of wireless communication*. Cambridge university press, 2005.
- [22] I. Goodfellow, Y. Bengio, and A. Courville, *Deep Learning*. MIT Press, 2016.
- [23] T. Gruber, S. Cammerer, J. Hoydis, and S. ten Brink, "On Deep Learning-Based Channel Decoding," in *Proc. of CISS*, Jan. 2017, pp. 1–6.
- [24] K. Simonyan and A. Zisserman, "Very deep convolutional networks for large-scale image recognition," *arXiv preprint arXiv:1409.1556*, Sept. 2014.
- [25] G. Y. Li, "Pilot-symbol-aided channel estimation for OFDM in wireless systems," in *1999 IEEE 49th Vehicular Technology Conference*, May 1999.
- [26] G. Cybenko, "Approximation by superpositions of a sigmoidal function," *Mathematics of control, signals and systems*, Feb. 1989.
- [27] USRP User Manual, Ettus Research. [Online]. Available: <https://www.ettus.com/>
- [28] M. Arnold, J. Hoydis and S. ten Brink, "Novel Massive MIMO Channel Sounding Data Applied to Deep Learning-based Indoor Positioning," *SCC 2019*, Feb.